CRITICAL CONJUNCTION DETECTION AND MITIGATION

Saika Aida[(1)], **Michael Kirschner**[(2)]
[(1)(2)]*DLR German Space Operations Center (GSOC) Oberpfaffenhofen, 82234 Weßling, Germany*
[(1)]*+49 8153 28-2158, saika.aida@dlr.de*
[(2)]*+49 8153 28-1385, michael.kirschner@dlr.de*

Abstract: *Criteria for the critical conjunction are discussed. In the current collision avoidance operation, the collision probability is a key parameter for the criticality assessment of the detected conjunction to decide an avoidance maneuver. The conventional probability threshold of ~10^{-4} has been applied for LEO conjunctions at the German Space Operations Center. However, not all conjunctions can be decided only by this criterion due to the large variation of the orbit uncertainties estimated for the numerous space objects. To evaluate the effect of this characteristic, the collision probability and the avoided risk for the probability threshold were formulated using the standard deviations related to the covariance ellipse projected onto the B-plane, which is perpendicular to the relative velocity. The encountering objects of the past conjunctions were also categorized by the same parameter. The avoidable conjunction was then evaluated in terms of the operational aspects. Finally, the collision risk as a result of the collision avoidance operation was assessed.*

Keywords: *Collision Probability, Avoided Risk, Standard Deviations.*

1. Introduction

At the German Space Operations Center (GSOC), 12 satellites in LEO, 8 satellites in MEO, and 2 satellites in GEO are currently supported in the collision avoidance system, to avoid a potential catastrophic collision against other space objects. Numerous conjunctions are daily reported, which are detected within certain distance thresholds.

In the conjunction risk assessment, the collision probability is one of the key parameters for the criticality evaluation, which leads to a detection of possible critical conjunctions or an avoidance maneuver decision. Several studies have been done concerning the collision probability threshold for a decision of an avoidance maneuver, which are based on the debris flux model [1] [2]. In the GSOC collision avoidance operation, a probability threshold of ~10^{-4} has been applied to an avoidance maneuver decision for LEO conjunctions. However, not all conjunctions can be decided only by this criterion due to the large variation of the orbit uncertainties estimated for the numerous space objects. For appropriate and effective conjunction mitigation, additional criteria are required even for the conjunctions with a higher collision probability.

In this paper, the fundamental equations are first shown, then the past conjunction results are presented and evaluated based on the equations. The size of the standard deviations derived from the positional covariance matices of encountering objects is used as a parameter to characterize the conjunction. The avoidable conjunction is then discussed in terms of the operational aspects such as avoided risk and area, and avoidance maneuver size. Finally the annual collision risk as a result of the collision avoidance operation is assessed.

2. Fundamental Equations

2.1. Collision Probability Calculation

Several methods for the collision probability calculation for the short-term encounter have been developed. The accuracy of some models was also compared and validated [3]. In the current general methods, the collision probability is calculated based on the hitradius and the orbital states and covariance information at the time of the closest approach (TCA). The hitradius is defined as a sum of each object radius and the shape is considered as a sphere, so that the object attitude at the conjunction is not taken into account. The position uncertainty is described by a 3D Gaussian distribution, and the velocity uncertainty is neglected. The position uncertainty of two objects is assumed to be uncorrelated. For the short-term encounter, two objects are assumed to be moving along straight lines at constant velocities, and the position uncertainty during the encounter is also assumed to be constant. Using these assumptions, the collision probability mapped onto the B-plane is expressed as Eq. 1 [4]. The B-plane is perpendicular to the relative velocity vector at TCA.

$$P_c = \frac{1}{2\pi \cdot \sqrt{det(C_B)}} \cdot \int_{-Rc}^{Rc} \int_{-\sqrt{Rc^2 - x^2}}^{\sqrt{Rc^2 - x^2}} exp\left[-\frac{1}{2} \Delta \hat{r}_B{}^T C_B{}^{-1} \Delta \hat{r}_B \right] dydx \tag{1}$$

R_c is the hitradius centered at the predicted fly-by location. $\Delta \hat{r}_B$ and C_B represent the projected position vector and covariance matrix. The maximum collision probability can be also calculated by scaling the covariance matrix by a factor k^2 [5]:

$$P_{c,max} = \frac{R_c{}^2}{exp(1)\sqrt{det(C_B)} \cdot \Delta \hat{r}_B{}^T C_B{}^{-1} \Delta \hat{r}_B} \tag{2}$$

$$k^2{}_{p\,max} = \frac{1}{2} \Delta \hat{r}_B{}^T C_B{}^{-1} \Delta \hat{r}_B \tag{3}$$

For a very small covariance ellipse, the relative position is far away from the ellipse center, which results in the small collision probability. As the covariance ellipse size increases, the probability reaches a maximum. Further increment of the covariance ellipse size leads to a dilution in the probability computation [6]. In such cases the maximum probability Eq. 2 is applied instead of the unscaled probability Eq. 1 so that the collision probability is not underestimated due to the larger orbit uncertainties.

2.2. Collision Probability Expressed by Covariance Scaling Factor

When the B-plane axes are aligned with the minor/major axes of the projected covariance ellipse and the probability is assumed to be constant within the integration radius, Eq. 1 and Eq. 2 can be written in the following forms:

$$P_c = \frac{R_c^{\,2}}{2 \cdot \sigma_x \sigma_y} \cdot exp\left[\left(-\frac{1}{2}\right) \cdot l^2\right] \tag{4}$$

$$P_{c,max} = \frac{R_c^{\,2}}{exp(1) \cdot \sigma_x \sigma_y} \cdot \frac{1}{l^2} \tag{5}$$

$$l^2 = \left\{\left(\frac{x_m}{\sigma_x}\right)^2 + \left(\frac{y_m}{\sigma_y}\right)^2\right\} \tag{6}$$

x_m and y_m are the respective components of the projected miss distance, and σ_x and σ_y are the corresponding standard deviations. Note that Eq. 6 indicates that the projected relative position lies along the scaled covariance ellipse with a factor of l.

2.3. Cumulative Probability inside Scaled Covariance Ellipse

For the Gaussian distribution, the cumulative probability inside a scaled covariance ellipse with minor/major axes of X/Y can be expressed as follows:

$$P_{inside\_ellip} = \frac{1}{2\pi \cdot \sigma_x \sigma_y} \cdot \int_{-X}^{+X} \int_{-Y}^{+Y} exp\left[-\frac{1}{2}\left\{\left(\frac{x}{\sigma_x}\right)^2 + \left(\frac{y}{\sigma_y}\right)^2\right\}\right] dydx \tag{7}$$

Using the scaling parameter defined in Eq. 6, it can be defined by the following equation.

$$P_{inside\_ellip} = 1 - exp\left(-\frac{l^2}{2}\right) \tag{8}$$

3. Avoided Risk Evaluation

3.1. Avoided Risk for Collision Probability Threshold

The equations Eq. 4, Eq. 5, and Eq. 8 indicate that the cumulative probability P_{inside_ellip} inside a probability contour ellipse $PoC=const$ is defined by the hitradius and the product of standard deviations $\sigma_x\sigma_y$ in the B-plane. In other words, the avoided risk for a certain probability threshold for the collision avoidance can be calculated for a given hitradius and standard deviations in the B-plane.

The avoided risk for corresponding probability thresholds for operational satellites are shown in Figure 1 for TerraSAR-X and TanDEM-X (at an altitude of 510 km, maximum length of 5.2 m) and in Figure 2 for ComsatBW-1&2 (in the geostationary orbit, maximum length of 17.2 m). The plot lines were generated for different size of standard deviations in the B-plane (0.01 km^2 ≤ $\sigma_x\sigma_y$ ≤ 0.5 km^2), and additionally the number of the expected conjunction per year. The number of conjunctions was estimated from the object population in the orbit and the size of the probability

contour ellipse. For the population calculation, the MASTER-2009 (Meteoroid And Space debris Terrestrial Environment Reference) Model was used. Man-made objects up to 10 m diameter are included in the population. The flux value in lower orbits varies greatly depending on the minimum size. It was estimated by a comparison with the operational conjunction results, and the lower threshold of 3 cm was selected [7]. The parameters used for the simulation are listed in Table 1.

Figure 1 shows that more than 99% of the risk is avoided at the probability threshold of 10^{-6} for $\sigma_x\sigma_y \leq 0.1$ km^2. However the number of the conjunction is more than 10 per year. At the conventional probability threshold of 10^{-4}, the avoided risk varies depending on the $\sigma_x\sigma_y$ value, and the avoided risk is below 10% in case of $\sigma_x\sigma_y \geq 0.5$ km^2. For GEO, Figure 2 shows that more than 99% of the risk is avoided at the probability threshold of 10^{-6} up to $\sigma_x\sigma_y \leq 0.5$ km^2, which covers broader standard deviations compared to Figure 1 due to the larger hitradius. The number of the conjunction is less than once per year due to the much less population in the geostationary orbit compared to the lower one as Table 1 shows. At the probability threshold of 10^{-4}, the avoided risk is higher than 80% for $\sigma_x\sigma_y \leq 0.1$ km^2, and drops below 30% at $\sigma_x\sigma_y \geq 0.5$ km^2.

Table 1 Hitradius and Flux Parameters

Orbit	Hitradius [m]	Flux [1/m^2/yr]	Flux period	Object diameter [m]
LEO (510 km)	5.0	1.204×10^{-5}	2014.01.01-2015.01.01	0.03 – 10.0
GEO	10.0	1.222×10^{-8}	2014.01.01-2015.01.01	1.00 – 10.0

3.2. Estimation of Standard Deviations in B-plane

The realistic value of $\sigma_x\sigma_y$ at the criticality decision was analyzed from the past conjunctions, using the Conjunction Data Message (CDM) analysis results for the operational satellites. When a CDM is received, the prediction is updated using the satellite orbit data and the covariance information. Orbit uncertainties of the operational satellites are based on the past analysis results derived from the satellite orbit data [8] [9]. The conjunction data for TerraSAR-X, TanDEM-X and ComsatBW-1&2 in 2013-2015 was used. The $\sigma_x\sigma_y$ value depends on the covariance matrices of two objects given at TCA and additionally the approach angle of the conjunction. Since the covariance matrix varies according to the propagation length, the conjunctions predicted close to the timing of the criticality decision were selected, which correspond to the CDMs generated during 0.5-1.5 days before TCA for LEO. For GEO satellites, the variation of the propagated covariance matrix is much smaller due to no influence of the atmosphere, therefore the CDMs generated during 0.5-3.0 days before TCA were used for the analysis. When multiple CDMs were available concerning a single conjunction, the latest one was selected. In total, 209 conjunctions were analyzed for LEO and 13 for GEO.

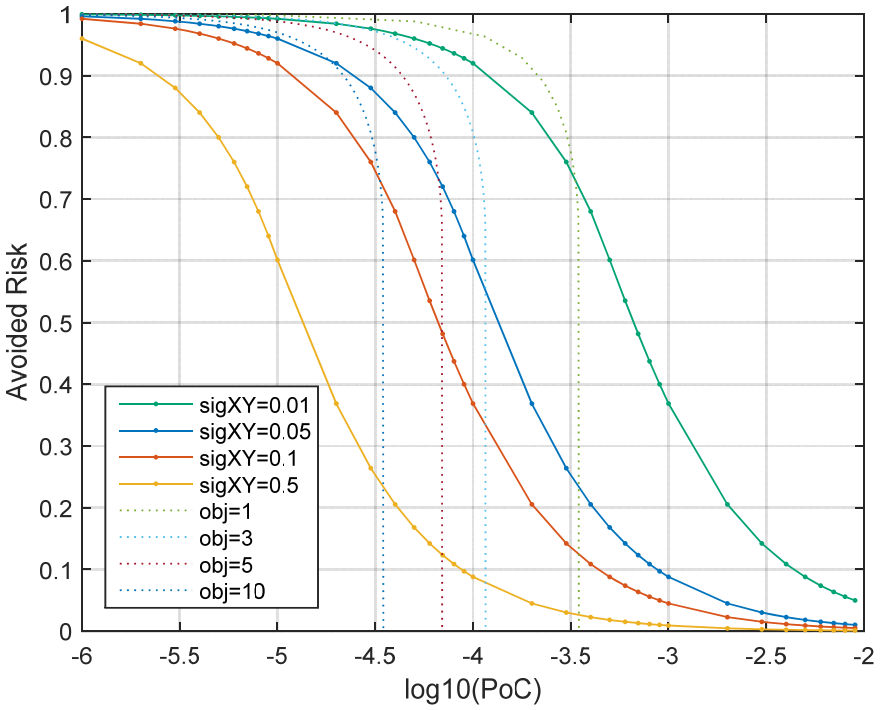

Figure 1 Avoided Risk for Probability Threshold (LEO, 510 km)

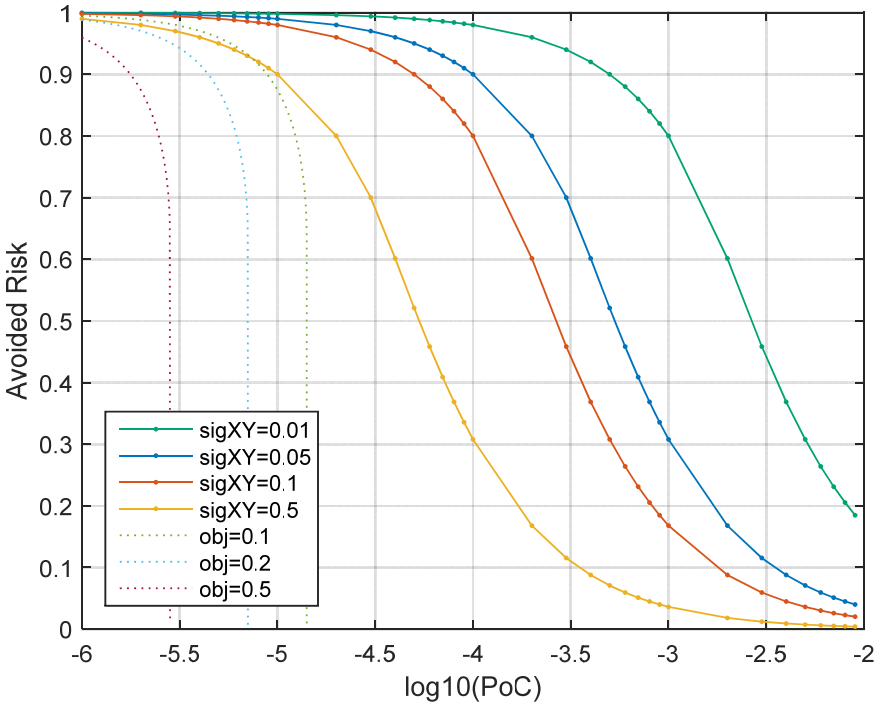

Figure 2 Avoided Risk for Probability Threshold (GEO)

The cumulative percentage and the number of the conjunction sorted by $\sigma_x\sigma_y$ values are shown in Figure 3 and Table 2. 95% of the conjunctions were $\sigma_x\sigma_y \leq 10$ km^2 for LEO, and all conjunctions were $\sigma_x\sigma_y \leq 1.0$ km^2 for GEO. For both orbits, more than 90% of the conjunctions were $\sigma_x\sigma_y \leq 0.5$ km^2. The upper dispersion of the $\sigma_x\sigma_y$ value is assumed to be less for the GEO conjunctions due to the detectable object size (> a few centimeters for LEO, > ~1 m for GEO) and the limited approach angle of the GEO conjunction, since the orbital inclination of the objects near the geostationary ring grow up to ~15 degrees due to the perturbation.

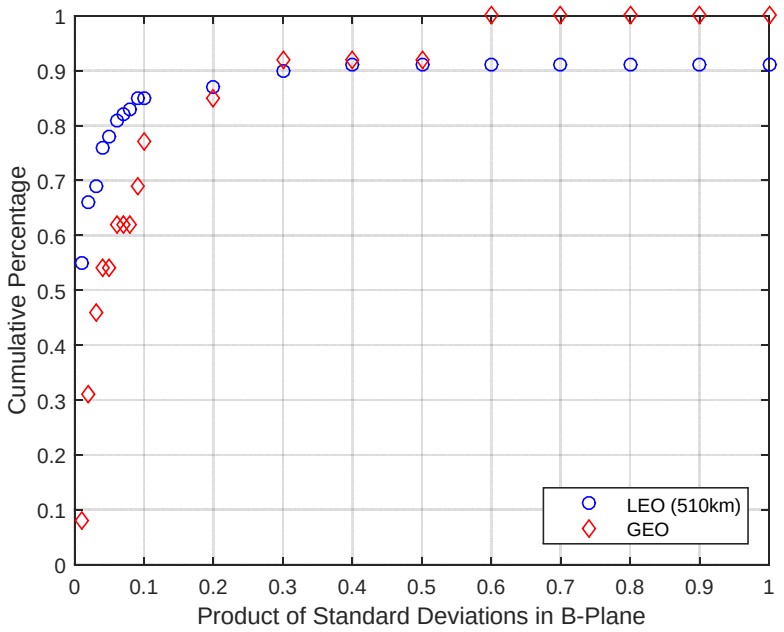

Figure 3 Cumulative Percentage of Conjunctions with Different Standard Deviations

Table 2 Conjunctions Sorted by Standard Deviations

$\sigma_x\sigma_y$ [km^2]	≤ 0.01	≤ 0.05	≤ 0.1	≤ 0.5	≤ 1	≤ 10	Total
LEO, 510 km (Sep.2014-Aug.2015)	115 (0.55)	163 (0.78)	178 (0.85)	190 (0.91)	191 (0.91)	199 (0.95)	209 (1.00)
GEO (Sep.2013-Aug.2015)	1 (0.08)	7 (0.54)	10 (0.77)	12 (0.92)	13 (1.00)	13 (1.00)	13 (1.00)

As Table 2 shows, 85% of the conjunctions in LEO had $\sigma_x\sigma_y$ values of ≤ 0.1 km^2. The remaining cases with $\sigma_x\sigma_y > 0.1$ km^2 are listed in Table 3. This table shows objects together with the radar cross section, perigee and apogee altitudes, orbit uncertainties (1σ) in RTN, the angle of two orbital planes, and the corresponding value of $\sigma_x\sigma_y$. Most objects are assumed to be relatively small debris with a diameter of ~10 cm. For a few cases, the higher eccentricity is considered as an additional reason for the worse accuracy i.e. SL-12 DEB. On the other hand, the orbit accuracies are partly better compared to others i.e. PSLV DEB, however the product of the standard deviations in the B-plane resulted in the higher value due to the smaller approach angle.

Table 3 Conjunctions with Higher Standard Deviations

dT [day]	ID	Name	RCS [m^2]	Peri [km]	Apo [km]	Err.R [km]	Err.T [km]	Err.N [km]	Angle [km^2]	$\sigma_x\sigma_y$ [km^2]
$0.1 < \sigma_x\sigma_y \leq 1.0$										
0.7	30748	FENGYUN_1C_DEB	0.014	510	562	0.096	7.016	0.018	68.1	0.13
1.3	37323	COSMOS_2251_DEB	0.010	515	628	0.187	4.246	0.042	156.7	0.16
1.0	27530	PSLV_DEB	0.013	451	512	0.091	2.668	0.022	85.8	0.18
0.8	34855	COSMOS_2251_DEB	0.006	516	539	0.071	3.486	0.070	54.1	0.20
1.4	18911	DIAMANT_DEB	0.016	504	865	0.080	4.990	0.027	107.4	0.23
1.3	31982	FENGYUN_1C_DEB	0.010	492	740	0.219	18.050	0.038	151.7	0.23
1.4	39001	CZ-2C_DEB	0.087	394	523	0.275	16.811	0.005	7.7	0.25
1.2	25809	SL-12_DEB	0.025	453	12242	0.629	7.485	0.129	107.7	0.37
1.3	31920	FENGYUN_1C_DEB	0.015	499	774	0.294	5.625	0.081	139.8	0.57
$1.0 < \sigma_x\sigma_y \leq 10.0$										
1.2	30861	FENGYUN_1C_DEB	0.010	498	557	0.187	16.384	0.048	83.8	1.38
1.0	87188	UNKNOWN	n/a	462	733	1.486	6.711	1.126	159.8	1.42
1.3	29787	FENGYUN_1C_DEB	0.032	454	526	0.675	48.462	0.027	122.8	1.51
1.0	37979	COSMOS_2251_DEB	0.014	490	738	0.210	9.739	0.475	23.8	1.54
0.9	34821	COSMOS_2251_DEB	0.012	465	513	0.312	18.048	0.427	30.1	3.30
$10.0 < \sigma_x\sigma_y$										
1.4	32108	FENGYUN_1C_DEB	0.011	428	518	1.070	729.579	0.115	118.1	39.41
0.8	80528	UNKNOWN	n/a	456	520	1.163	406.894	0.073	9.8	47.44
0.9	36168	FENGYUN_1C_DEB	0.013	507	608	5.148	1567.875	0.247	155.4	71.21
0.5	81152	UNKNOWN	n/a	501	539	0.685	338.083	0.340	11.4	154.04
0.8	36024	IRIDIUM_33_DEB	0.005	494	733	0.948	695.089	0.134	51.6	212.72

3.3. Avoided Risk for Past Conjunctions

The avoided risk and the collision probability for past conjunctions of TerraSAR-X and TanDEM-X during the period of December 2013 - November 2014 are plotted in Figure 4. The analysis results of CDMs generated up to 2 days before TCA were selected. The conjunctions which evoked an avoidance maneuver planning and execution are additionally marked with x. In the collision avoidance operation at GSOC, conjunctions with the probability higher than or close to 10^{-4} were closely analyzed, and the decision of the avoidance maneuver was made ~1 day before TCA. Since the satellites perform orbit control maneuvers frequently, the planned maneuver was only adjusted to reduce the risk for a few cases. The lines for different size of standard deviations and the number of the expected conjunction per year as in Figure 1 are also plotted. In the operational process, the collision probability is calculated using a default radius of 2.0 m for the objects with an unknown size. Since most encountering objects have an unknown or similar size, the hitradius of ~5.0 m is applicable for most conjunctions.

Figure 4 shows that most of the higher risk conjunctions with $PoC > 5.0\times10^{-5}$ resulted in an avoided risk lower than 0.7 due to the limited orbit accuracy. Some events were ignored because of the too large orbit errors, which lead to the avoided risk closer to zero. Compared with the

expected object number, the operational results show less events, which can be explained by the flux difference and the number of samples taken from a year statistics.

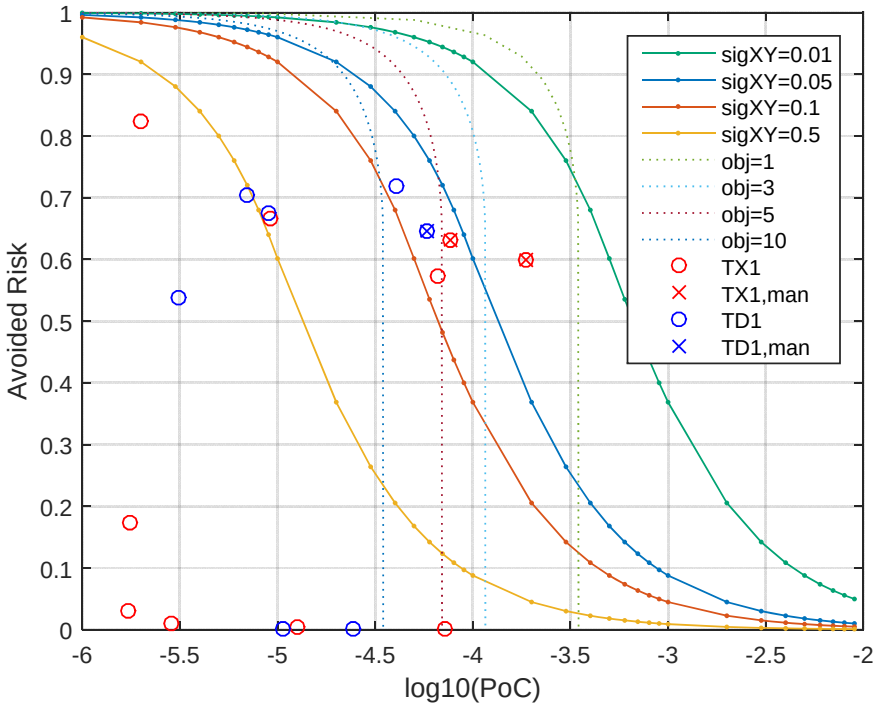

Figure 4 Avoided Risk and Collision Probability for Past Conjunctions (TerraSAR-X and TanDEM-X, Dec. 2013 - Nov. 2014)

4. Criteria for Avoidable Conjunction

4.1. Avoided Risk and Avoided Area

As Figure 4 shows, the avoided risk for the high risk conjunctions varies greatly depending on the standard deviations in the B-plane. At the conventional maneuver threshold of 10^{-4}, conjunctions only with smaller standard deviations of $\sigma_x\sigma_y \leq 0.01$ km^2 achieve an avoided risk higher than 0.9, which is only 55% of the encountering objects at 510 km altitude according to Table 2. To handle the remaining objects, the probability threshold needs to be adjusted, the object accuracy needs to be improved i.e. by additional tracking, or part of the objects with high $\sigma_x\sigma_y$ values shall be ignored to avoid an ineffective avoidance maneuver.

At the lower probability threshold, the avoided risk gets higher but the corresponding probability contour line expands. Since conjunctions inside this ellipse result in higher probabilities than the threshold value, such conjunctions shall be avoided. Therefore, the lower threshold leads to a larger exclusion zone and accordingly a larger number of avoided conjunctions. Figure 5 shows the relation between the avoided risk and the avoidance area concerning different standard deviations and collision probabilities. Avoided area was calculated as the product of the semi-minor and the semi-major axes of the corresponding ellipse. The number of conjunctions

expected for the corresponding avoided area is listed in Table 4. The same flux values as in Table 1 were used for the calculation.

When the collision probability threshold is lowered to 5.0×10^{-5}, the avoided risk increases up to 0.6 for $\sigma_x\sigma_y$ = 0.1 km^2. On the other hand, the risk still remains below 0.2 for $\sigma_x\sigma_y$ = 0.5 km^2, which is less effective to avoid or needs improvement of the orbit accuracy. The avoided area reaches 0.184 km^2, which corresponds to a circle of 430 m radius, when the ratio of the standard deviations is 1. When the ratio is 5, it corresponds to the total distance of ~960 m, and the quasi-radial distance of ~190 m in the B-plane. It should be mentioned that the direction of the semi-minor axis is near to the radial direction for most conjunctions. In both cases, the number of the expected conjunction is 7 per year according to Table 4.

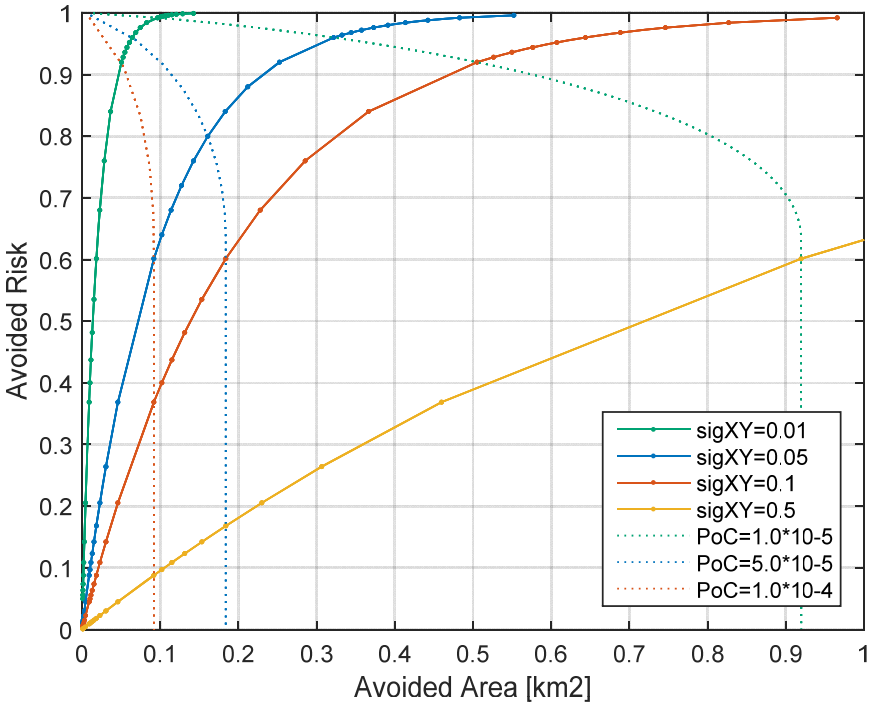

Figure 5 Avoided Risk and Avoided Area (Hitradius=5.0 m)

Table 4 Annual Conjunctions for Avoided Area

Orbit	Flux [1/m^2/yr]	Avoided Area [km^2]					
		0.05	0.1	0.2	0.3	0.5	1.0
LEO (510 km)	1.204×10^{-5}	1.9	3.8	7.6	11.3	18.9	37.8
GEO	1.222×10^{-8}	0.002	0.004	0.008	0.012	0.019	0.038

4.2. Estimation of Avoidance Maneuver Size

The maneuver size for the collision avoidance was estimated for different probability thresholds. The typical collision avoidance maneuver, which has been already applied to the operational

LEO satellites, is to increase the radial separation by an intrack thrusting half an orbit before the closest approach. A certain separation can be achieved in a short period and also with a relatively small maneuver in this way. Additionally, the satellite can easily come back to the nominal orbit shortly after the closest approach. To estimate the maneuver size in case of the same maneuver strategy, the required radial separation was calculated from the difference between two probability contour ellipsoids at each semi-minor axis, which is nearly parallel to the radial direction of the primary satellite for most conjunctions. The ratio of the standard deviations was assumed to be 3, although the value varies greatly depending on the conjunction. It shall be noted that the smaller ratio close to 1 leads to the larger radial separation. The goal of the collision probability after the avoidance maneuver was set so that a remaing risk of 0.05 or 0.01 is achieved. The maneuver size to achieve the separation was calculated from the following equation, where ΔD_R is the increment of the radial separation, a is the semi-major axis, and V is the velocity:

$$\Delta a = \frac{\Delta D_R}{2} \approx 2 \cdot \frac{\Delta V}{V} \cdot a \tag{9}$$

Figure 6 shows the maneuver size to reach a remaing risk of 0.05 and 0.01 respectively. At a collision probability of 10^{-4}, a remaing risk of 0.05 can be achieved by a maneuver of < 8 cm/s for $\sigma_x\sigma_y \leq 0.1$ km^2, whereas more than 20 cm/s is required for $\sigma_x\sigma_y \geq 0.5$ km^2. Additionally, the target collision probability to reach the remaing risk of 0.01 is between 10^{-6} and 10^{-5} for $\sigma_x\sigma_y \leq 0.1$ km^2, and nearly 10^{-7} for $\sigma_x\sigma_y = 0.5$ km^2.

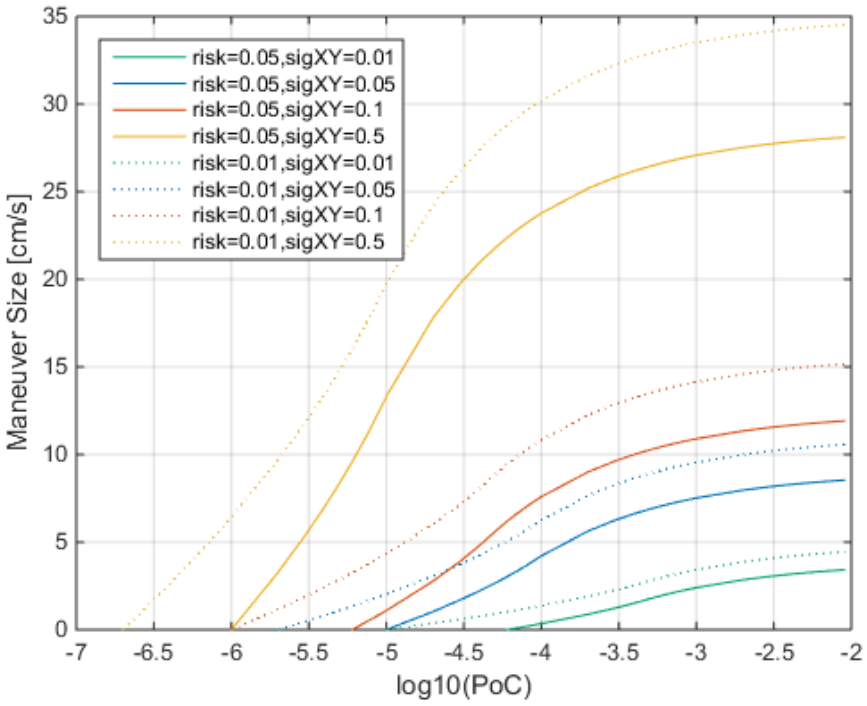

Figure 6 Maneuver Size to Reach 95% and 99% Ellipse (Hitradius=5.0 m, AR=3)

5. Annual Collision Risk Estimation

The remaining collision risk as a result of the collision avoidance operation was estimated.
The annual collision risk for a satellite is the sum of the fluxes of the individual encountering objects, multiplied by the area of the combined object dimension. It also corresponds to the integral out to infinity of the collision probability per unit area associated with constant collision probability contours [1]. Among the annual collision risk, the avoided one is the integral out to the contour line concerning the collision probability threshold of $P=Pm$:

$$P_A = \sum_j F_j A_C = \sum_j \int_{A=0}^{\infty} PF_j dA = \sum_j \int_{A=0}^{A(Pm)} PF_j dA + \sum_j \int_{A(Pm)}^{\infty} PF_j dA \tag{10}$$

P_A is the annual collision risk, A_C is the area of the combined dimension, and F_j is the annual flux of the j-th object group. The object group was categorized by the value of the product of the standard deviations in the B-plane according to the operational results as shown in Table 2. For different cases of the avoided object, the average size of the $\sigma_x\sigma_y$ value was calculated, and the remaining risk for different collision probability thresholds was estimated. Table 5 shows the parameters used for each avoidance case. The same hitradius and flux values as in Table 1 were used for the calculation.

Figure 7 shows the annual collision risk for the different avoidance cases. The broken line shows the total annual collision risk of 9.46×10^{-4}. When only the objects with $\sigma_x\sigma_y \leq 0.01$ km^2 are avoided, the avoided rate is higher than other lines for the higher probability threshold; however the remaining risk becomes almost constant and higher than other cases below the probability threshold of 10^{-4}. The reason is that only 55% of the population can be avoided according to Table 5. To decrease the remaining risk, the objects with higher $\sigma_x\sigma_y$ values shall be additionally avoided. When the objects with $\sigma_x\sigma_y \leq 0.50$ km^2 are avoided, the remaining risk is nearly 10% of the expected total risk at the threshold of 10^{-6}, whereas it increases the number of the avoidance maneuver and the maneuver size as discussed in section 4. To lower the still remaining risk, the orbit accuracy of mostly small objects with higher $\sigma_x\sigma_y$ values as shown in Table 3 need to be improved by additional tracking. In the collision avoidance operation at GSOC, a short-term tracking campaign for orbit refinement is planned using the Tracking and Imaging Radar (TIRA). However the trackable objects and the achieved accuracy need to be investigated.

Table 5 Avoided Object Group and Parameters

	LEO (510 km)		GEO	
$\sigma_x\sigma_y$ size of avoided objects [km^2]	Population percentage	Average $\sigma_x\sigma_y$ [km^2]	Population percentage	Average $\sigma_x\sigma_y$ [km^2]
≤ 0.01	0.55	0.003	0.08	0.008
≤ 0.05	0.78	0.010	0.54	0.020
≤ 0.10	0.85	0.014	0.77	0.038
≤ 0.50	0.91	0.027	0.92	0.058

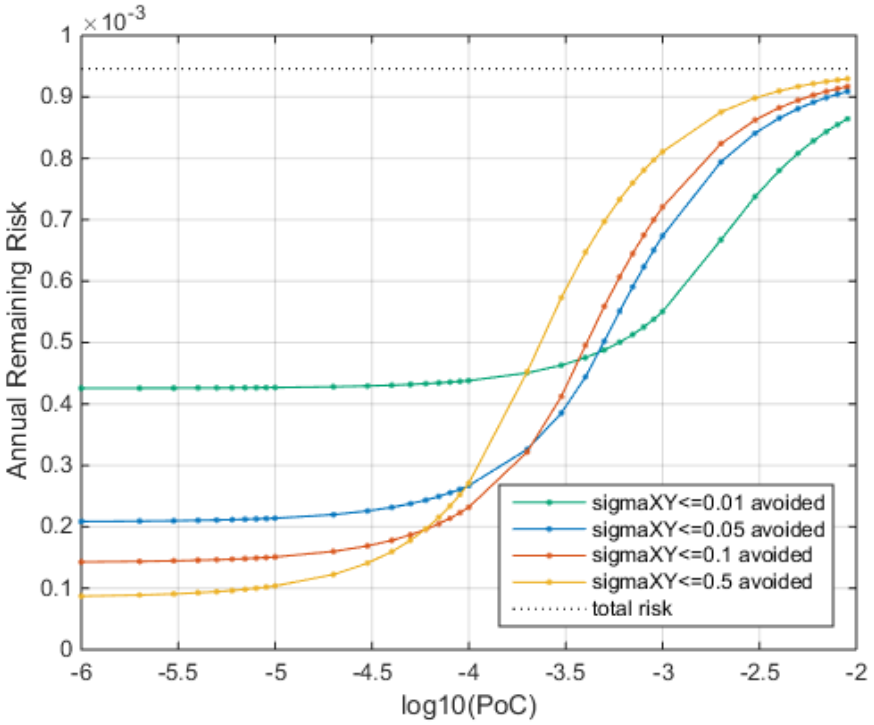

Figure 7 Remaining Risk (Hitradius=5.0 m, LEO, 510 km)

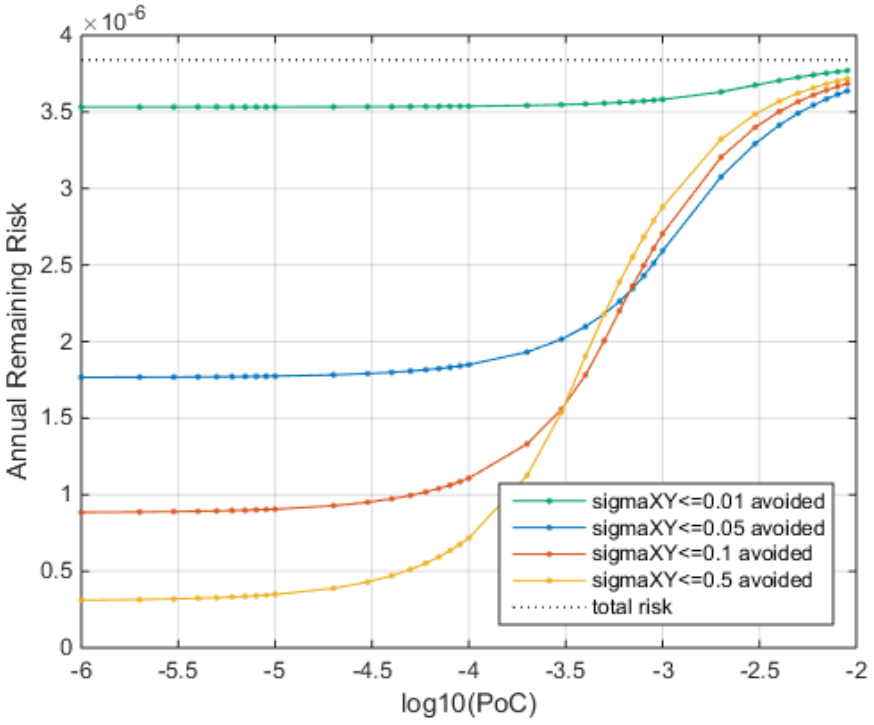

Figure 8 Remaining Risk (Hitradius=10.0 m, GEO)

The remaining risk for GEO is shown in Figure 8. Despite of the larger hitradius, the total risk of 3.84×10^{-6} is much lower than the LEO case due to the lower flux value. Compared with Figure 7, the achievable avoided risk is very small for $\sigma_x\sigma_y \leq 0.01$ km^2. When the objects with $\sigma_x\sigma_y \leq 0.50$ km^2 are avoided, the remaining risk is nearly 10% of the total risk at the threshold of 10^{-6}; however, the maneuver size shall be carefully analyzed to keep the geostationary satellite in the control box.

6. Conclusion

To derive the criteria for the critical conjunction with the high collision probability, the collision probability and the avoided risk for the probability threshold were formulated using the standard deviations related to the covariance ellipse projected onto the B-plane. The encountering objects of the past conjunctions were also categorized by the same parameter. The avoidable conjunction was then evaluated in terms of the avoided risk and area, maneuver frequency, and avoidance maneuver size. In case of the larger $\sigma_x\sigma_y$ value, the avoided risk is lower for the same collision probability threshold, and the avoided area becomes larger for the same avoided risk, which leads to a larger number of the avoided conjunction especially in the populated area in LEO. Additionally the maneuver size to achieve the acceptable remaining risk increases. Such encountering objects ($\sigma_x\sigma_y > \sim0.1$ km^2) are mostly small objects in LEO, therefore orbit refinement using additional tracking is required or the conjunction shall be ignored to avoid the ineffective avoidance maneuver. The trackable objects and the achieved accuracy need to be further investigated. Finally, the annual conjunction risk as a result of the collision avoidance operation was assessed for different avoided objects categorized by the $\sigma_x\sigma_y$ value.

7. References

[1] Foster, J. “The Analytic Basis for Debris Avoidance Operations for the International Space Station.” Proceeding of the Third European Conference on Space Debris, ESA SP-473. 2001.

[2] Klinkrad, H., Alarcon, J., and Sanchez, N. “Collision Avoidance for Operational ESA Satellites.” Proceeding of the Fourth European Conference on Space Debris, ESA SP-587. 2005.

[3] Alfano, S. “Review of Conjunction Probability Methods for Short-term Encounters.” AAS/AIAA Paper 07-148.

[4] Foster, J. and Estes, H. “A Parametric Analysis of Orbital Debris Collision Probability and Maneuver Rate for Space Vehicles.” NASA/JSC-25898 August 1992.

[5] Alfriend, K., Akella, M., Lee, D., Frisbee, J., Foster, J., Lee, D., and Wilkins, M. “Probability of Collision Error Analysis.” Space Debris Vol. 1 No. 1 (1999) pp. 21-35 Springer.

[6] Alfano, S. “Relating Position Uncertainty to Maximum Conjunction Probability.” AAS/AIAA Paper 03-548.

[7] Aida, S. “Collision Probability Threshold Analysis.” DLR/GSOC TN 14-12. 2014.

[8] Aida, S. and Kirschner, M. “Collision Risk Assessment and Operational Experiences for LEO Satellites at GSOC.” 22nd International Symposium on Spaceflight Dynamics Sao Jose dos Campos, Brazil. Feb. 28 - Mar. 4. 2011.

[9] Aida, S. “Orbit Accuracy Analysis of GEO Satellites.” DLR/GSOC TN 14-02. 2014.